Regulation of Neurabin I Interaction with Protein Phosphatase 1 by Phosphorylation†

Thomas McAvoy,‡ Patrick B. Allen,§ Hiroshi Obaishi,|| Hiroyuki Nakanishi,|| Yoshimi Takai,⊥ Paul Greengard,§ Angus C. Nairn,§ and Hugh C. Hemmings, Jr.*,‡,§

Departments of Anesthesiology and Pharmacology, Weill Medical College of Cornell University, New York, New York 10021, Laboratory of Molecular and Cellular Neuroscience, The Rockefeller University, New York, New York 10021, Takai Biotimer Project, ERATO, Japan Science and Technology Corporation, Kobe 651-22, Japan, and Department of Molecular Biology and Biochemistry, Osaka University School of Medicine, Suita 565, Japan

Received May 28, 1999; Revised Manuscript Received August 9, 1999

ABSTRACT: Neurabin I is a brain-specific actin-binding protein. Here we show that neurabin I binds protein phosphatase 1 (PP1) and inhibits PP1 activity. Neurabin I interacted with PP1α in an overlay assay, in yeast two-hybrid interaction analysis, and in coprecipitation and co-immunoprecipitation experiments. Neurabin I also copurified with both the α and γ isoforms of PP1. A glutathione *S*-transferase (GST)−neurabin I fusion protein (residues 318−661) containing the putative PP1 binding domain (residues 456−460) inhibited PP1 activity ($K_i = 2.7 \pm 1.2$ nM). This fusion protein was also rapidly phosphorylated in vitro by PKA ($K_m = 6$ μM) to a stoichiomtry of 1 mol/mol. The phosphorylated residue was identified as serine 461 by HPLC−MS analysis of a tryptic digest. Phosphorylation of GST−neurabin I (residues 318−661) by PKA significantly reduced its binding to PP1 by overlay and by glutathione−Sepharose coprecipitation assays. A 35-fold decrease in inhibitory potency was also observed using a S461E mutant, which mimics phosphorylation of S461. These findings identify a signaling mechanism involving the regulation of PP1 activity and localization mediated by the cAMP pathway.

Protein kinases and phosphatases act cooperatively to regulate many neuronal processes (for reviews, see refs *1*−*4*), including receptor and ion channel function (*5*, *6*), neurotransmitter release (*7*), and synaptic plasticity (*8*, *9*). Many protein kinases and phosphatases exist in complexes with targeting or anchoring subunits (for a review, see ref *10*), which act to concentrate the enzymes in subcellular compartments near their substrates and sites of action and thus influence the specificity and integration of regulated signaling networks.

Dephosphorylation of proteins phosphorylated on seryl/threonyl residues involves several major phosphatases, including protein phosphatase 1 (PP1)[1] (*11*). PP1 interacts with a variety of proteins that control both its subcellular distribution and, in many instances, its activity (*12*). In brain, a significant amount of the PP1 is present in an inactive state, presumably bound to inhibitory regulatory and targeting subunits (*13*, *14*). Three PP1 isoforms (α, β, and γ1) are expressed in brain (*15*). Of these, α and γ1 are concentrated in dendritic spines (*16*) where they apparently play an important role in dephosphorylating substrates such as the postsynaptic density (PSD)-associated Ca^{2+}/calmodulin-dependent protein kinase II (*17*).

Neurabin I is a neural tissue-specific F-actin binding protein (*18*) which is homologous to spinophilin (also known as neurabin II), a PP1 targeting subunit that is highly concentrated in dendritic spines (*19*). The two proteins share features, including an N-terminal F-actin binding domain, a central PDZ domain, and a C-terminal coiled-coil domain (*19*, *20*). They also share significant sequence similarity in a large central domain that is implicated in PP1 binding and modulation of PP1 activity (*21*, *22*). Unlike spinophilin, neurabin I contains an extended C terminus which includes additional coiled-coil domains and a SAM (sterile-alpha motif) domain, which may mediate additional protein interactions (*23*). In the study presented here, we examined the interactions of neurabin I with PP1 and its regulation by phosphorylation.

EXPERIMENTAL PROCEDURES

Materials. Microcystin-LR was obtained from Calbiochem (La Jolla, CA) and conjugated to 4% beaded agarose by the

† This work was supported in part by National Institutes of Health Grants MH 40899 and DA 10044 and the Department of Anesthesiology, Weill Medical College of Cornell University.

* To whom correspondence should be addressed: Department of Anesthesiology, Box 50, Weill Medical College of Cornell University, 525 E. 68th St., New York, NY 10021. Telephone: (212) 746-2714. Fax: (212) 746-8316. E-mail: hchemmi@mail.med.cornell.edu.

‡ Weill Medical College of Cornell University.

§ The Rockefeller University.

|| Japan Science and Technology Corporation.

⊥ Osaka University School of Medicine.

[1] Abbreviations: PP1, protein phosphatase 1; $PP1_C$, catalytic subunit of PP1; $PP2A_C$, catalytic subunit of protein phosphatase 2A; PDZ, consensus sequence in PDZ95/DLG/zo-1; SAM, sterile-alpha motif; GST, glutathione *S*-transferase; NIPP-1, nuclear inhibitor of PP1; G_M, glycogen-binding subunit of PP1 from striated muscle; G_L, glycogen-binding subunit of PP1 from liver; DARPP-32, dopamine- and cAMP-regulated phosphoprotein, with an M_r of 32 000; SDS−PAGE, sodium dodecyl sulfate−polyacrylamide gel electrophoresis; PKA, cyclic AMP-dependent protein kinase; PMSF, phenylmethanesulfonyl fluoride; PSD, postsynaptic densities; HPLC, high-performance liquid chromatography; MS, mass spectrometry; ECL, enhanced chemiluminescence.

10.1021/bi991227d CCC: $18.00 © 1999 American Chemical Society
Published on Web 09/09/1999

method of Moorhead et al. (*24*). Phosphorylase *b*, phosphorylase kinase, and *N*-hydroxysuccinimidylagarose were from Sigma Chemical Co. (St. Louis, MO). [^{125}I]Protein A and [^{32}P]ATP were from NEN (Boston, MA). Protein G−Sepharose, glutathione−Sepharose, goat anti-GST antibodies, and the ECL immunoblotting detection system were from Amersham-Pharmacia (Arlington Heights, IL). The micro BCA protein assay kit was from Pierce (Rockford, IL). Modified trypsin was from Promega (Madison, WI). Purified recombinant CK1 and CK2 were obtained from New England Biolabs (Beverly, MA). Purified rabbit muscle PP1 ($PP1_C$), protein phosphatase 2A ($PP2A_C$), and bacterially expressed PP1α were provided by H. B. Huang (The Rockefeller University). Purified rabbit anti-PP1α antibodies (RU34) were prepared as described previously (*15*) or obtained from Upstate Biotechnology Inc. (Lake Placid, NY). Rabbit anti-spinophilin antibodies (RU145) were raised against a synthetic peptide corresponding to residues 367−390 of spinophilin and purified as described previously (*19*). Rabbit anti-neurabin I antiserum raised against GST−neurabin I amino acids 486−751 (*25*) was kindly provided by P. Burnett and S. Snyder (Johns Hopkins School of Medicine, Baltimore, MD). Purified rabbit anti-neurabin I antibodies raised against GST−neurabin I amino acids 609−868 were prepared as described previously (*18*).

Purification of PP1 Binding Proteins. Adult male Sprague-Dawley rats (150−200 g) were anesthetized with 80% CO_2/20% O_2 and sacrificed. The cerebral cortex and striatum from 10 rats were dissected and homogenized together in 5 volumes of ice-cold homogenization buffer [320 mM sucrose, 1 mM EDTA, 1 mM EGTA (pH 7.5), 0.1% (v/v) β-mercaptoethanol, 1 mM benzamidine, 10 μg/mL leupeptin, 10 μg/mL pepstatin, and 1 mM phenylmethanesulfonyl fluoride (PMSF)] with eight strokes in a glass/Teflon homogenizer at 900 rpm. After centrifugation at 2200*g* for 2 min, the supernatant (S1) was transferred to a new tube and centrifuged at 39000*g* for 20 min to yield supernatant (S2) and pellet (P2) fractions. The P2 fraction (crude synaptosomes) was resuspended in 4 volumes of lysis buffer [5 mM Tris-HCl (pH 7.5), 1 mM EDTA, 1 mM EGTA, 0.1% β-mercaptoethanol, 1 mM benzamidine, 10 μg/mL leupeptin, 10 μg/mL pepstatin, and 1 mM PMSF] with the aid of a glass/Teflon homogenizer, and incubated on ice for 1 h. After centrifugation at 39000*g* for 20 min, the supernatant (lysed P2 soluble fraction) was applied to a Mono Q 10/10 column (Pharmacia) equilibrated with buffer A [20 mM Tris-HCl (pH 7.7), 1 mM EDTA, 1 mM benzamidine, and 0.1% β-mercaptoethanol]. After washing with 30 mL of buffer A, 4 mL fractions were collected over an 80 mL linear gradient from 250 to 600 mM NaCl in buffer A with a flow rate of 4 mL/min. Fractions containing PP1 binding proteins (analyzed by the PP1 overlay assay) were pooled and further purified on a microcystin−agarose column (1.5 cm × 8 cm, 10 mL). After washing with 20 mL of buffer A containing 100 mM NaCl, binding proteins were eluted in 5 mL of buffer A containing 3 M NaSCN. The eluate was concentrated and desalted into buffer A using a centrifugal ultrafiltration device (Millipore) before analysis by sodium dodecyl sulfate−polyacrylamide gel electrophoresis (SDS−PAGE).

PP1 Overlay and Immunoblotting. Protein samples were boiled for 5 min in SDS loading buffer [10% (w/v) sucrose, 2% (w/v) SDS, 0.01% (v/v) β-mercaptoethanol, and 62.5 mM Tris-HCl (pH 6.8)], separated by SDS−PAGE by the method of Laemmli (*26*), transferred as described by Towbin et al. (*27*) to 0.2 μm nitrocellulose membranes (Schleicher & Schuell), and incubated overnight in blocking solution [10 mM sodium phosphate (pH 7.2), 150 mM NaCl, 0.5% (v/v) Tween 20, and 2.5% (w/v) Carnation dried milk]. For PP1α overlay (far Western) analysis, blots were incubated with 1.5 μg/mL bacterially expressed PP1α in blocking solution for 90 min. After washing for 3 × 5 min with blocking solution, blots were probed with anti-PP1α antibody (1:500 dilution in blocking solution) for 90 min. Blots were washed for 3 × 5 min, and immunoreactive protein bands were detected with [^{125}I]protein A (≈0.1 μCi/mL in blocking solution) for 90 min followed by washing for 3 × 30 min with blocking solution. Anti-spinophilin and anti-neurabin I immunoblots were incubated with primary antibody in blocking solution [1.5 μg/mL anti-spinophilin antibodies (RU145) or a 1:100 dilution of antiserum against GST−neurabin I (amino acids 486−751)] for 90 min and washed for 3 × 5 min in blocking solution before detection with [^{125}I]protein A. Immunoreactive bands were visualized by autoradiography and quantified by PhosphorImager analysis (Molecular Dynamics).

Copurification of PP1 with Neurabin I. A "synaptic soluble" fraction was prepared from rat cerebral cortex as described previously (*28*), which is similar to the "lysed P2 soluble" fraction described above, except an additional density centrifugation step was performed before lysis to enrich the sample in synaptic proteins. Neurabin I was purified from this fraction by successive chromatographic steps using Q-Sepharose, phenyl-Sepharose, hydroxylapatite, Mono Q, and Mono S columns as described previously (*18*). Following the Mono S column purification step, fractions containing neurabin I were separated by SDS−PAGE, and a protein band appearing as a doublet with an approximate M_r of 36 kDa was visualized with Coomassie Brilliant Blue. These protein bands were separately excised and digested with lysyl endopeptidase. The proteolytic products were separated by reverse phase high-pressure liquid chromatography (HPLC), and the amino acid sequences were determined by peptide microsequencing as described previously (*18*).

Co-Immunoprecipitation of Neurabin I with PP1. CHAPS was added to a portion of the synaptic soluble fraction to give a final concentration of 0.6% (w/v). Samples (200 μg of protein each) were incubated with rabbit anti-PP1α antibodies (Upstate Biotechnology Inc.) or normal rabbit IgG (2 μg each) at 4 °C for 3 h. Protein G−Sepharose beads (20 μL) were added, and the mixture was incubated for an additional 1 h. The beads were washed three times with PBS [10 mM sodium phosphate (pH 7.2) and 150 mM NaCl], and bound proteins were eluted by boiling in SDS sample buffer. Proteins were separated by SDS−PAGE (8% acrylamide) followed by immunoblot analysis using an antibody against GST−neurabin I (amino acids 609−868). Immunoreactive bands were detected by ECL.

Yeast Two-Hybrid Analysis. The yeast two-hybrid interaction assay was performed as previously described (*29*). Bait vectors, pBTM116-neurabin-I-1 (amino acids 1−430), pBTM116-neurabin-I-2 (amino acids 431−760), pBTM116-neurabin-I-3 (amino acids 761−1095), pBTM116-neurabin-

I-4 (amino acids 453−630), and pBTM116-neurabin-I-5 (amino acids 461−630), were constructed by subcloning neurabin I inserts into *Eco*RI−*Sal*I sites of pBTM116. A yeast two-hybrid library constructed from adult rat brain cDNA was screened by β-galactosidase expression as described previously (*29*).

Preparation of GST−Neurabin I and Mutagenesis. The DNA sequence encoding neurabin I residues 318−661 was subcloned into the *Sal*I−*Not*I sites of pGEX-4T-2 (Pharmacia), which directs expression of a fusion protein with an N-terminal glutathione *S*-transferase (GST). This construct was also used as a template for site-directed mutagenesis using the Stratagene Quickchange site-directed mutagenesis kit. All mutations were confirmed by DNA sequencing.

All fusion proteins were produced in *Escherichia coli* BL21 cells essentially as described previously (*30*). GST fusion proteins were purified by affinity chromatography on glutathione−Sepharose beads (6 mL), eluted with 10 mM glutathione and 50 mM Tris-HCl (pH 8.0), and concentrated and desalted using ultrafiltration devices (Amicon). Protein concentrations were determined by the bicinchoninic acid (BCA) method (*31*) and adjusted for purity, as assessed by Coomassie Brilliant Blue R-250 staining of gels and densitometry scanning.

Phosphatase Activity Measurements. Purified rabbit skeletal muscle $PP1_C$ and $PP2A_C$ were analyzed for inhibition by GST−neurabin I (residues 318−661) using [^{32}P]phosphorylase *a* as a substrate as described previously (*32*). PP1 activity measurements in the presence of 100 mM KCl were modified by increasing the reaction time to 30 min and using 3 times more $PP1_C$. K_i values were calculated by linear regression analysis (Pharm/PCS, version 4.2, Springer-Verlag, New York).

In Vitro Phosphorylation. GST−neurabin I (residues 318−661, 5 μM) was phosphorylated by the purified catalytic subunit of PKA {40 μg/mL in kinase buffer [50 mM Tris-HCl (pH 7.5), 10 mM $MgCl_2$, and 5 mM DTT]}, CK1 (10 units/μL in kinase buffer), or CK2 [5 units/μL in 20 mM Tris-HCl (pH 7.5), 50 mM KCl, and 10 mM $MgCl_2$] in the presence of [^{32}P]ATP or cold ATP. Aliquots taken at various time intervals were diluted into an equal volume of 2× SDS−PAGE loading buffer, separated by SDS−PAGE, and transferred to nitrocellulose. The extent of binding of PP1α to GST−neurabin I (residues 318−661) was determined by overlay analysis in the presence of 1 μM microcystin-LR to prevent dephosphorylation, with detection by [^{125}I]protein A and PhosphorImager analysis.

Identification of the PKA Phosphorylation Site. An in vitro phosphorylation reaction mixture containing GST−neurabin I (residues 318−661) and PKA was incubated with or without (control) ATP for 1 h at 30 °C; with ATP, a stoichiometry of 1 mol/mol was obtained. GST−neurabin I was purified with glutathione−Sepharose, desalted with a Bio-spin 6 column (Bio-Rad), and digested with sequencing grade modified trypsin in 50 mM NH_4HCO_3 (pH 7.8) and 10% acetonitrile overnight at 37 °C. Peptides were separated by HPLC and analyzed by ESI-MS/MS (WMC core facility) to identify the fragment(s) containing phosphate.

In Vitro Coprecipitation Experiments. GST−neurabin I (residues 318−661) or phospho-GST−neurabin I (1 μM) was incubated for 5 min with various concentrations of bacterially expressed PP1α at 4 °C in PBS. Glutathione−Sepharose beads (5 μL) were then added and allowed to bind for 3 min while the mixture was being shaken. The liquid was removed, and the beads were washed with 1 mL of cold PBS. The beads were boiled in 2× SDS−PAGE loading buffer and loaded on 10% polyacrylamide gels. Separated proteins were transferred to nitrocellulose and immunoblotted with both anti-GST antibodies and anti-PP1α antibodies.

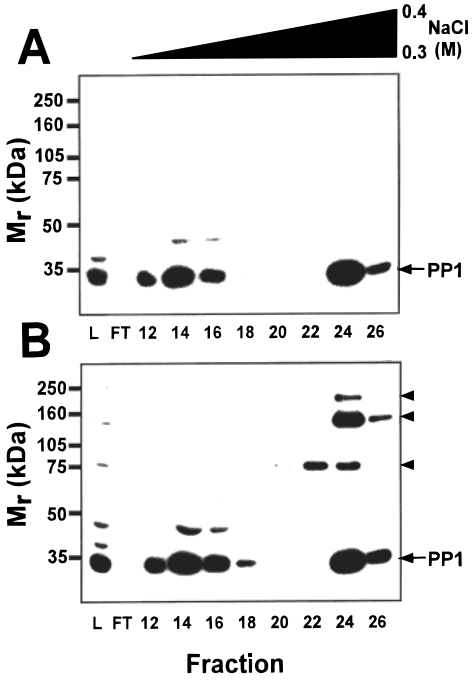

FIGURE 1: Ion-exchange fractionation of PP1α binding proteins. A lysed P2 soluble fraction prepared from rat cortex and striatum was separated by FPLC using a Mono Q anion-exchange column with a linear gradient from 250 to 600 mM NaCl. Aliquots from even-numbered fractions, the load (L), and flow-through (FT) were analyzed by SDS−PAGE (10% acrylamide, 20 μL/lane) and transferred to nitrocellulose. Panel A shows an anti-PP1α immunoblot of fractions 12−26. PP1α overlay analysis of the same fractions is shown in panel B. PP1α binding proteins, identified as bands detected in the overlay but not in the anti-PP1α immunoblot, are denoted with arrowheads.

RESULTS

PP1 Binding Proteins in Brain. Anion-exchange chromatography of proteins in the lysed P2 soluble fraction (low-ionic strength extract of crude synaptosomes) revealed two major peaks of PP1α immunoreactivity (Figure 1). A major peak of PP1α eluted between 300 and 350 mM NaCl (fractions 12−18), and a second peak of PP1α eluted between 380 and 400 mM NaCl (fractions 24−26). Overlay (far Western) analysis, involving incubation of nitrocellulose gel transfers with purified PP1α followed by anti-PP1α immunoblotting, was used to identify PP1 binding proteins which may be responsible for this differential elution. Bands appearing in the overlay blot (Figure 1B), but not in the control anti-PP1α immunoblot (Figure 1A), were identified as PP1α binding proteins. Two proteins (M_r = 135 and 180 kDa) coeluted with the second PP1α peak. Another protein (M_r = 75 kDa) that eluted between 370 and 390 mM NaCl (fractions 22−24) partially overlapped the second peak of PP1α immunoreactivity.

The PP1α binding proteins in anion-exchange fractions 24−26 were further purified by affinity chromatography with microcystin−agarose, which retains protein complexes con-

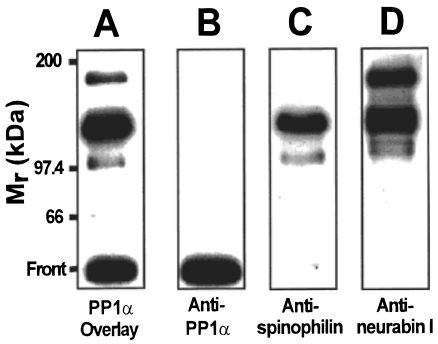

FIGURE 2: Identification of spinophilin and neurabin I as PP1 binding proteins. Fractions from the Mono Q anion-exchange column containing the second peak of PP1α immunoreactivity and PP1α binding proteins (fractions 24−26) were pooled and purified by microcystin−agarose affinity chromatography. Bound proteins were separated by SDS−PAGE (6% acrylamide), transferred to nitrocellulose, and analyzed by (A) PP1α overlay, (B) anti-PP1α immunoblot (overlay control), (C) anti-spinophilin immunoblot, and (D) anti-GST neurabin I (residues 486−751) immunoblot analysis.

taining either PP1 or PP2A via a strong interaction which involves the active site (*24*, *33*, *34*). PP1α binding proteins purified with microcystin−agarose and eluted with 3 M NaSCN were separated by SDS−PAGE and analyzed by PP1α overlay analysis (Figure 2A) and by immunoblotting with specific antibodies (Figure 2B−D). Both the 180 and 135 kDa proteins, but not the 75 kDa protein, were detected in the eluate by PP1α overlay analysis. The 135 kDa protein was identified as spinophilin by its apparent M_r on SDS−PAGE and by immunoblotting (Figure 2C). Similarly, the 180 kDa protein was identified as neurabin I by its apparent M_r on SDS−PAGE and by immunoblotting with an antiserum against GST−neurabin I (amino acids 486-751), which also cross-reacted with spinophilin (Figure 2D). Both antibody preparations also recognized lower-molecular mass bands assumed to be breakdown products of spinophilin (≈100 kDa) or neurabin I (≈140 kDa).

Copurification of PP1 with neurabin I and spinophilin was also observed after five successive chromatographic steps used to purify neurabin I and spinophilin from the synaptic soluble fraction (low-ionic strength extract of purified synaptosomes). Two protein bands appearing as a doublet ($M_r \approx 36$ kDa; Figure 3A) that coeluted with neurabin I were digested with lysyl endopeptidase and sequenced individually. Peptides LNLDSIIGRLLEVQGSRPGK and DVQGWGENDRGVSFTFGAEVVAK corresponding to PP1α amino acids 7−26 and 212−234, respectively, were obtained from the upper band. Peptides SREIFLSQPILLELEAP and DVLGWGENDRGVSFTFGAEVVAK corresponding to PP1γ amino acids 42−58 and 212−234, respectively, were obtained from the lower band. Interaction between neurabin I and PP1 was confirmed by co-immunoprecipitation. Neurabin I was detected by immunoblotting after immunoprecipitation of PP1α from the synaptic soluble fraction (Figure 3B).

Neurabin I−PP1 Interaction. In an independent search for proteins which interact with neurabin I, 2×10^7 yeast transformants prepared from a rat brain cDNA library were screened by the two-hybrid analysis using a mixture of three bait constructs: pBTM-neurabin-I-1, pBTM-neurabin-I-2, and pBTM-neurabin-I-3. One clone that was recovered (pPrey A) contained a 1.3 kb insert that encoded PP1α (amino acids 3−330, data not shown). The minimal region

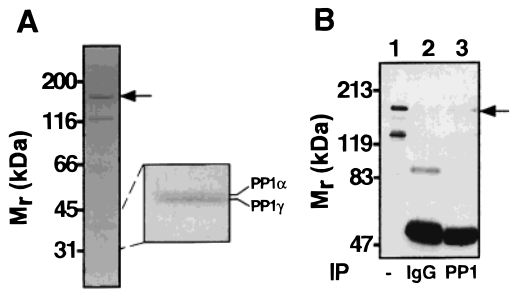

FIGURE 3: Copurification and co-immunoprecipitation of PP1 and neurabin I. (A) The α and γ isoforms of PP1 are copurified with neurabin I. Following purification of neurabin I (arrow) from the rat cerebral cortex synaptic soluble fraction, two copurifying bands at 36 kDa were visualized by protein staining. The bands were excised and individually analyzed by proteolysis and peptide microsequencing and identified from their amino acid sequences as PP1α and PP1γ, as indicated. The left panel shows a peak fraction of neurabin I eluting from a Mono S column and separated on a 8 to 15% polyacrylamide gel. The smaller panel, right, shows a similar fraction separated on a 8 to 20% gel, to enhance resolution of the two bands. (B) Co-immunoprecipitation. The synaptic soluble fraction (lane 1) was immunoprecipitated with 2 μg of control IgG (lane 2) or 2 μg of anti-PP1α antibody (lane 3), separated by SDS−PAGE, and subjected to anti-GST−neurabin I (residues 608−868) immunoblot analysis detected by ECL. The arrow denotes neurabin I immunoreactivity (180 kDa). The ∼50 kDa band represents nonspecific staining of the IgG heavy chain.

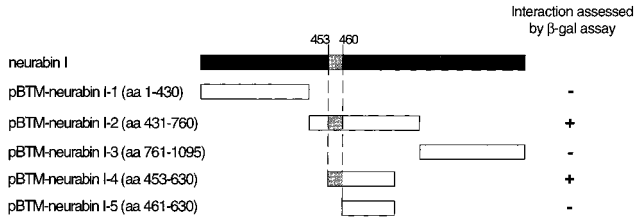

FIGURE 4: Identification of the PP1 binding domain of neurabin I by yeast two-hybrid interaction analysis. Plasmids expressing fragments of neurabin I were transformed into yeast together with pPrey A (PP1α), and interactions were evaluated by β-galactosidase expression screening. The diagram is not to scale.

of neurabin I required for interaction with PP1 was also examined. Retransformation of fresh yeast cells with these constructs individually showed that pPrey A bound to pBTM-neurabin-I-2, but not to pBTM-neurabin-I-1 or pBTM-neurabin-I-3 (Figure 4). The truncated constructs, pBTM-neurabin-I-4 and pBTM-neurabin-I-5, were similarly tested. pPrey A interacted with pBTM-neurabin-I-4, but not with pBTM-neurabin-I-5. This indicates the importance of amino acids 453−460 in the interaction with PP1α.

GST−neurabin I (amino acids 318−661), which contains residues 453−460 identified by the yeast two-hybrid analysis as critical for the PP1α interaction, bound PP1α by overlay analysis (Figure 5A). Using [^{32}P]phosphorylase *a* as the substrate, GST−neurabin I (amino acids 318−661) inhibited purified rabbit muscle $PP1_C$ with an IC_{50} of 0.2 ± 0.06 nM (Figure 5B). The activity of the PP2A catalytic subunit was only slightly affected (<15% inhibition at 1 μM). Kinetic analysis of inhibition data on a double-reciprocal plot reveals a noncompetitive mechanism of inhibition with a K_i value of 2.7 ± 1.2 nM (Figure 5C).

Phosphorylation of GST−neurabin I (amino acids 318−661) by purified kinases was analyzed in vitro. CK1, CK2, and cyclic AMP-dependent kinase (PKA) rapidly phosphorylated this fragment of neurabin I (Figure 6A). Both CK1

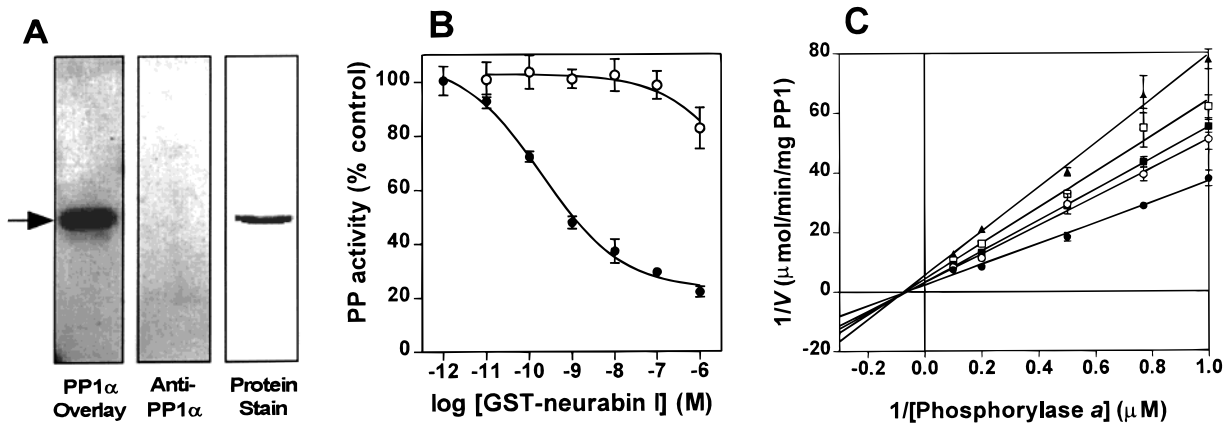

FIGURE 5: Neurabin I binds and inhibits PP1. (A) Purified GST−neurabin I (amino acids 318−661, 0.45 μg) interacts with PP1α by overlay analysis, but is not detected by anti-PP1α immunoblot analysis (overlay control). A sample of the purified fusion protein (1.2 μg) stained with Coomassie Brilliant Blue R-250 is also shown. (B) Effects of purified GST−neurabin I (amino acids 318−661) on $PP1_C$ (●) and $PP2A_C$ (○) catalytic activity using [^{32}P]phosphorylase *a* as the substrate. Results are calculated as percent activity (mean ± SD) in the absence of added fusion protein (n = 3). (C) Lineweaver−Burk plot for analyzing the inhibition of $PP1_C$ phosphorylase *a* activity by GST−neurabin I (residues 318−661) at 0 (●), 0.5 (○), 1 (■), 2 (□), and 5 nM (▲).

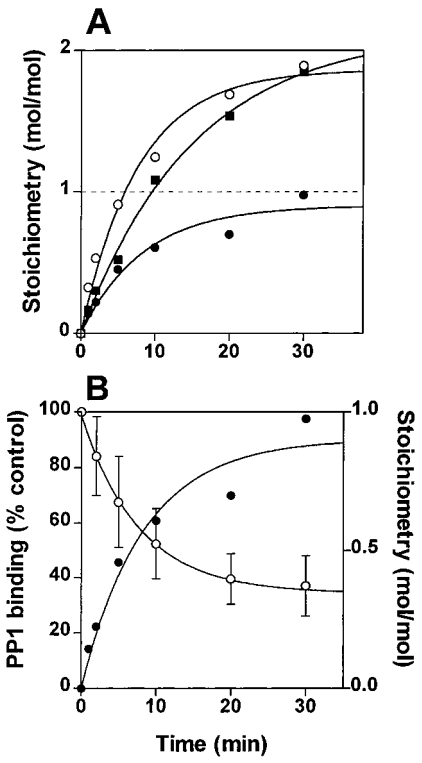

FIGURE 6: In vitro phosphorylation of GST−neurabin I (amino acids 318−661) by various protein kinases. (A) Time course of phosphorylation by PKA (●), CK1 (○), or CK2 (■). (B) The increase in the extent of phosphorylation of GST−neurabin I by PKA (●) paralleled the percent decrease in the extent of PP1 binding determined by overlay analysis (○).

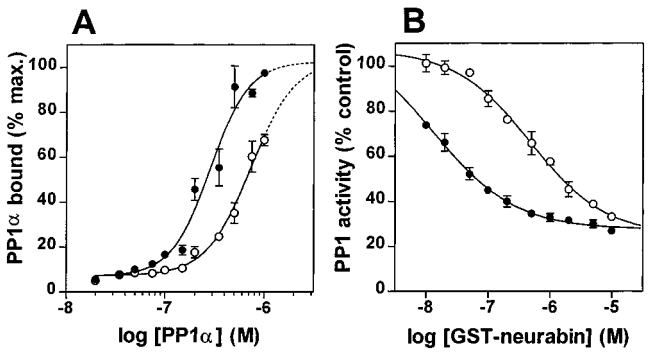

FIGURE 7: Phosphorylation of GST−neurabin I (amino acids 318−661) by PKA decreases the level of interaction with PP1. (A) Coprecipitation experiment comparing the abilities of 100 nM dephospho-GST−neurabin I (●) and phospho-GST−neurabin I (○) to bind various concentrations of PP1α. Dephosphorylation of GST−neurabin I was minimized by separating bound proteins after incubation for 5 min at 4 °C. (B) $PP1_C$ activity measurements at physiologic ionic strength (PP1 assay buffer and 100 mM KCl) using [^{32}P]phosphorylase *a* as the substrate comparing wild-type GST−neurabin I (●) and the phosphoserine mimic S461E (○). The S461E mutant was used to avoid the dephosphorylation seen with PKA-phosphorylated GST−neurabin under assay conditions (30 °C for 10 min).

and CK2 phosphorylated GST−neurabin I to an apparent stoichiometry of 2 mol/mol, while PKA phosphorylated the fragment to a stoichiometry of 1 mol/mol. Protein kinase C and Ca^{2+}/calmodulin-dependent kinase II (CaMKII) did not phosphorylate this fragment. Kinetic studies showed that GST−neurabin I (amino acids 318−661) was phosphorylated by PKA with a K_m value of 6 μM and a V_{max} of 0.11 μmol min^{-1} mg^{-1}. GST−neurabin I (amino acids 318−661) was phosphorylated to a stoichiometry of 1 mol/mol by PKA and digested with trypsin. HPLC−MS analysis determined that the major site of phosphorylation was serine 461. Analysis of PP1α binding by the overlay assay revealed a significant decrease after PKA treatment. This decrease paralleled the increase in the level of phosphorylation by PKA (Figure 6B). PP1 binding was not affected by phosphorylation by CK1 or CK2.

The effect of phosphorylation by PKA on the ability of GST−neurabin I (amino acids 318−661) to interact with PP1α was also analyzed by a glutathione−Sepharose coprecipitation assay (Figure 7A). Phosphorylation by PKA reduced the affinity of GST−neurabin I (amino acids 318−661) for PP1α as indicated by the rightward shift in the binding isotherm. Under the conditions of this assay, no significant dephosphorylation of [^{32}P]phospho-GST−neurabin I (amino acids 318−661) was detected. Scatchard analysis of the coprecipitation data determined that the K_D for PP1 binding to GST−neurabin I (amino acids 318−661) is approximately 110 nM (data not shown).

PP1 activity measurements were used to examine the consequences of phosphorylation at serine 461 on the ability

	species		reference
neurabin I	rat	453 P A N R K I K F S C A 463	U72994
spinophilin	rat	444 A P S R K I H F S I A 454	AFO16252
inhibitor 1	rat	5 N S P R K I Q F T V P 15	JO5592
DARPP-32	rat	4 K D R K K I Q F S V P 14	M27444
G_L	rat	57 K V K K R V S F A D N 67	S80360
G_M	rabbit	61 S G G R R V S F A D N 71	M65109
NIPP-1	bovine	196 R K N S R V T F S E D 206	Z50748

FIGURE 8: Amino acid sequence comparison of putative PP1 binding motifs from several known PP1 binding proteins. Boxed residues indicate the conserved PP1 binding motif. Highlighted serines are putative PKA phosphorylation sites which are proposed regulatory sites for influencing interaction with PP1. References are to GenBank accession numbers.

of neurabin I (residues 318−661) to inhibit $PP1_C$. A serine 461 to glutamate mutant was constructed to mimic phosphorylation and eliminate interference with the assay by potential dephosphorylation of serine 461. This was necessary since phospho-GST−neurabin I (amino acids 318−661) was dephosphorylated by $PP1_C$ and large quantities of pure thiophospho-GST−neurabin I (amino acids 318−661) were difficult to produce. This mutant exhibited a decreased ability to bind PP1 in coprecipitation experiments, similar to that of the PKA phosphorylated protein (data not shown). Results using the S461E mutant demonstrate a shift in inhibitory potency without an effect on maximal inhibition when assayed at physiologic ionic strength (Figure 7B). The IC_{50} value increased from 13 ± 7 nM for the wild type to 478 ± 84 nM for the mutant, a 35-fold increase.

DISCUSSION

Neurabin I is a 180 kDa F-actin binding protein specific to neural tissue (*18*). Here we show that neurabin I also functions as a PP1 binding protein. It copurifies with PP1α and PP1γ through multiple chromatographic procedures, interacts with PP1α in an overlay assay and yeast two-hybrid screen, and potently inhibits the catalytic activity of PP1α. Spinophilin, a 130 kDa protein which is structurally related to neurabin I, also interacts with PP1 (*19*, *20*, *22*). Despite their similarities, unique physiological roles may exist for each. Neurabin I is expressed principally in neural tissue, whereas spinophilin is widely distributed in many tissues. They may also have distinct subcellular localizations in neurons. Spinophilin is highly concentrated in dendritic spines (*19*), whereas neurabin I has been suggested to be in the lamellipodia of the growth cone (*18*) and nerve terminals (*25*). The extended C-terminal coiled-coil domains and SAM domain on neurabin I suggest a distinct cytoskeletal role. Finally, differences in their consensus phosphorylation site sequences indicate distinct regulatory mechanisms via signaling pathways exist.

The yeast two-hybrid experiments implicate residues 453−460 of neurabin I as an essential region for interaction with PP1α. Examination of the amino acid sequence in this region reveals the presence of a (R/K)(R/K)(V/I)xF motif (amino acids 456−460; *35*) which is present in other known PP1 binding proteins (Figure 8). This binding motif appears to be necessary and sufficient for PP1 binding, although there is evidence that additional contacts with PP1 are necessary to achieve the nanomolar binding affinities seen with neurabin I and spinophilin (*22*). Sequences distinct from the RKVxF binding motif may also influence the modulation of PP1 activity. Structural analysis indicates that this motif interacts with PP1 at a site distinct from the active site (*35*). Also, a synthetic neurabin I peptide (amino acids 447−470) spanning this motif slightly potentiated, rather than inhibited, $PP1_C$ activity against phosphorylase *a* (unpublished observation). The noncompetitive mechanism of inhibition observed for neurabin I suggests no competitive interference with phosphorylase *a* binding. Furthermore, microcystin−Sepharose chromatography, which relies on an interaction of the toxin microcystin-LR with the active site of PP1, was able to purify PP1 bound to both neurabin I and spinophilin, suggesting an allosteric interaction. Thus, it is likely that an additional site on neurabin I, which presumably alters the substrate specificity of PP1, is required for inhibition of PP1 catalytic activity toward phosphorylase *a* without complete obstruction of the active site.

We also report regulation of the neurabin I−PP1 interaction involving phosphorylation of serine 461 of neurabin I by PKA. This residue is located immediately C-terminal to the PP1 binding motif (residues 456−460). Neurabin I is a good substrate for PKA, presumably due in part to three highly basic residues preceding serine 461 within the PP1 binding motif (*36*), although their presence at the −2, −4, and −5 positions is unusual. Phosphorylation in or near the PP1 binding motif apparently decreases the affinity of this site for PP1. Consistent with this hypothesis, phosphorylation by PKA inhibited the interaction between GST−neurabin (amino acids 318−661) and PP1α. A GST−neurabin I mutant (S461E) that mimics phosphorylation by PKA decreased inhibitory potency by 35-fold. Interestingly, this reduction in potency was only seen at physiologic ionic strength, similar to previous observations for NIPP-1 (*37*) and G_M (*38*), which are also phosphorylated by PKA at the PP1 binding motif, leading to a dissociation of $PP1_C$.

In cultured hippocampal neurons, neurabin I is concentrated at the growth cone and its expression is necessary to support neurite formation (*18*). Treatment with okadaic acid, an inhibitor of PP1 and PP2A, leads to a decrease in the level of neurite outgrowth (*39*), which is consistent with a significant role for PP1, and possibly neurabin I as a PP1 targeting subunit, in neurite outgrowth. Our results suggest that neurabin I directs PP1 to specific locations within the cell and regulates the localization and activity of PP1 under the control of the cyclic AMP/PKA system. The significance of this effect will be examined in future studies of the regulation of PP1 localization by neurabin I in intact cells. The physiological role of the PP1−neurabin I interaction will depend on the interaction and characterization of the neuronal substrates for PP1.

ACKNOWLEDGMENT

We thank P. Burnett and S. Snyder (Johns Hopkins School of Medicine) for the generous gift of anti-GST−neurabin I (residues 486−751) antiserum.

REFERENCES

1. Hemmings, H. C., Jr., Nairn, A. C., McGuinness, T. L., Huganir, R. L., and Greengard, P. (1989) *FASEB J. 3*, 1583−1592.
2. Nairn, A. C., and Shenolikar, S. (1992) *Curr. Opin. Neurobiol. 2*, 296−301.
3. Girault, J. A. (1993) *Neurochem. Int. 23*, 1−25.
4. Liu, J. (1997) *Clin. Exp. Pharmacol. Physiol. 24*, 611−618.

5. Surmeier, D. J., Bargas, J., Hemmings, H. C., Jr., Nairn, A. C., and Greengard, P. (1995) *Neuron 14*, 385−397.
6. Endo, S., Critz, S. D., Byrne, J. H., and Shenolikar, S. (1995) *J. Neurochem. 64*, 1833−1840.
7. Greengard, P., Valtorta, F., Czernik, A. J., and Benfenati, F. (1993) *Science 259*, 780−785.
8. Mulkey, R. M., Endo, S., Shenolikar, S., and Malenka, R. C. (1994) *Nature 369*, 486−488.
9. Blitzer, R. D., Connor, J. H., Brown, G. P., Wong, T., Shenolikar, S., Iyengar, R., and Landau, E. M. (1998) *Science 280*, 1940−1943.
10. Pawson, T., and Scott, J. D. (1997) *Science 278*, 2075−2080.
11. Wera, S., and Hemmings, B. A. (1995) *Biochem. J. 311*, 17−29.
12. Hubbard, M. J., and Cohen, P. (1993) *Trends Biochem. Sci. 18*, 172−177.
13. Colbran, R. J., Bass, M. A., McNeill, B., Bollen, M., Zhao, S., Wadzinski, B. E., and Strack, S. (1997) *J. Neurochem. 69*, 920−929.
14. Sim, A. T. R., Ratcliffe, E., Mumby, M. C., Villa-Moruzzi, E., and Rostas, J. A. P. (1994) *J. Neurochem. 62*, 1552−1559.
15. da Cruz e Silva, E. F., Fox, C. A., Ouimet, C. C., Gustafson, E., Watson, S. J., and Greengard, P. (1995) *J. Neurosci. 15*, 3375−3389.
16. Ouimet, C. C., da Cruz e Silva, E. F., and Greengard, P. (1995) *Proc. Natl. Acad. Sci. U.S.A. 92*, 3396−3400.
17. Strack, S., Barban, M. A., Wadzinski, B. E., and Colbran, R. J. (1997) *J. Neurochem. 68*, 2119−2128.
18. Nakanishi, H., Obaishi, H., Satoh, A., Wada, M., Mandai, K., Satoh, K., Nishioka, H., Matsuura, Y., Mizohuchi, A., and Takai, Y. (1997) *J. Cell Biol. 139*, 951−961.
19. Allen, P. B., Ouimet, C. C., and Greengard, P. (1997) *Proc. Natl. Acad. Sci. U.S.A. 94*, 9956−9961.
20. Satoh, A., Nakanishi, H., Obaishi, H., Wada, M., Takahashi, K., Satoh, K., Hirao, K., Nishioka, H., Hata, Y., Mizohuchi, A., and Takai, Y. (1998) *J. Biol. Chem. 273*, 3740−3475.
21. Kwon, Y. G., Huang, H. B., Desdouits, F., Girault, J. A., Greengard, P., and Nairn, A. C. (1997) *Proc. Natl. Acad. Sci. U.S.A. 94*, 3536−3541.
22. Hsieh-Wilson, L. C., Allen, P. B., Watanabe, T., Nairn, A. C., and Greengard, P. (1999) *Biochemistry 38*, 4365−4373.
23. Thanos, C. D., Goodwill, K. E., and Bowie, J. U. (1999) *Science 283*, 833−836.
24. Moorhead, G., MacKintosh, C., Morrice, N., and Cohen, P. (1995) *FEBS Lett. 362*, 101−105.
25. Burnett, P. E., Blackshaw, S., Lai, M. M., Qureshi, I. A., Burnett, A. F., Sabatini, D. M., and Snyder, S. H. (1998) *Proc. Natl. Acad. Sci. U.S.A. 95*, 8351−8356.
26. Laemmli, U. K. (1970) *Nature 227*, 680−685.
27. Towbin, H., Staehelin, T., and Gordon, J. (1979) *Proc. Natl. Acad. Sci. U.S.A. 76*, 4350−4354.
28. Mizoguchi, A., Kim, S., Ueda, T., Kikuchi, A., Yorifuji, H., Hirokawa, N., and Takai, Y. (1989) *J. Biol. Chem. 265*, 11872−11879.
29. Takeuchi, M., Hata, Y., Hirao, K., Toyoda, A., Irie, M., and Takai, Y. (1997) *J. Biol. Chem. 272*, 11943−11951.
30. Grieco, F., Hay, J. M., and Hull, R. (1992) *BioTechniques 13*, 856−858.
31. Smith, P. K., Krohn, R. I., Hermanson, G. T., Mallia, A. K., Gartner, F. H., Provenzano, M. D., Fujimoto, E. K., Goeke, N. M., Olson, B. J., and Klenk, D. C. (1985) *Anal. Biochem. 150*, 76−85.
32. Cohen, P., Alemany, S., Hemmings, B. A., Resink, T. J., Stralfors, P., and Tung, H. Y. (1988) *Methods Enzymol. 159*, 390−400.
33. Campos, M., Fadden, P., Alms, G., Qian, Z., and Haystead, T. A. J. (1996) *J. Biol. Chem. 271*, 28478−28484.
34. Goldberg, J., Huang, H. B., Kwon, Y. G., Greengard, P., Nairn, A. C., and Kuriyan, J. (1995) *Nature 376*, 745−753.
35. Egloff, M. P., Johnson, D. F., Moorhead, G., Cohen, P. T., Cohen, P., and Barford, D. (1997) *EMBO J. 16*, 1876−1887.
36. Kemp, B. E., Graves, D. J., Benjamini, E., and Krebs, E. G. (1977) *J. Biol. Chem. 252*, 4888−4894.
37. Vulsteke, V., Beullens, M., Waelkens, E., Stalmans, W., and Bollen, M. (1997) *J. Biol. Chem. 272*, 32972−32978.
38. Hubbard, M., and Cohen, P. (1989) *Eur. J. Biochem. 186*, 701−709.
39. Malchiodi-Albedi, F., Petrucci, T. C., Picconi, B., Iosi, F., and Falchi, M. (1997) *J. Neurosci. Res. 48*, 425−438.

BI991227D